Assessment of *Syzygium cumini* (Jamblang) fruit extract as an eco-friendly corrosion inhibitor for low-carbon steel in 3.5% NaCl medium

N. Ali,[1]* S. Fonna,[1] N. Nurdin,[2] Y. Saputra[1] and A.K. Arifin[3]

[1]*Department of Mechanical and Industrial Engineering, Universitas Syiah Kuala, Banda Aceh 23111, Indonesia*
[2]*Department of Electrical and Computer Engineering, Universitas Syiah Kuala, Banda Aceh 23111, Indonesia*
[3]*Department of Mechanical and Materials Engineering, Universiti Kebangsaan Malaysia, Bangi 43600, Selangor DE, Malaysia*
**E-mail: nurdin.ali@usk.ac.id*

Abstract

The use of environmentally friendly inhibitors, such as plant extract in preventing corrosion is an effective alternative to hazardous and toxic chemical additives. Therefore, this study aims to assess the effectiveness of an inhibitor derived from *Syzygium cumini* fruit extract on low carbon steel in a 3.5% NaCl corrosive medium. The extraction process was carried out using the solid-liquid method, and the extract obtained was characterized using Fourier Transfer Infrared Spectroscopy (FTIR) and phytochemical analysis. Corrosion inhibition properties were analyzed through weight loss measurement, electrochemistry (PDP), and electrochemical impedance spectroscopy (EIS). The surface morphology of the sample was examined using Scanning Electron Microscope-Energy Dispersive X-ray (SEM-EDX) and X-ray diffraction (XRD). The results showed the effectiveness of *Syzygium cumini* fruit extract in preventing corrosion at concentrations of 100, 200, 300, 400, and 500 ppm. The highest corrosion efficiency was approximately 92.99% at a concentration of 500 ppm. Furthermore, this result was validated by surface analysis based on the inhibitor adsorption process on low carbon steel. The high efficiency and minimal damage to the sample showed that *Syzygium cumini* fruit was an environmentally friendly inhibitor with excellent corrosion protection.

Received: December 14, 2023. Published: February 1, 2024 doi: 10.17675/2305-6894-2024-13-1-11

Keywords: *corrosion, Syzygium cumini, weight loss, potentiodynamic polarization, electrochemical impedance spectroscopy.*

1. Introduction

Corrosion is the gradual degradation of materials caused by direct exposure to a corrosive environment, leading to a decline in metal quality and disintegration [1]. This process is typically an electrochemical reaction occurring within an unstable thermodynamic system [2]. Furthermore, several studies have shown that it is influenced by various factors

including O_2 content, fluid velocity, pH level, stress, and the presence of chloride (Cl) compounds in water [3]. Carbon steel is a widely used metal in industrial construction, buildings, bridges, and everyday equipment due to its economic feasibility, strength, good thermal conductivity, and ductility. However, its application is limited due to poor resistance to aggressive environments, such as seawater containing sodium chloride (NaCl) compound [4].

According to previous studies, corrosion caused by NaCl deposits is influenced by the condensation process within the corrosive solution atmosphere, leading to an increased degradation rate [5]. The limited resistance of carbon steel in NaCl solutions is caused by the direct adsorption of Cl ions by the metal, thereby forming Cl ions on the surface [6]. Continuous corrosion occurs in metals that are naturally unstable and tend to electrochemically react with aggressive environments. Previous studies have reported that chloride ions can induce carbon steel corrosion at medium or high temperatures, such as in neutral seawater environments with NaCl [7] and in fuels containing KCl [8]. This process has also been reported to have adverse effects on materials, human safety, and the economy [9]. Therefore, protective applications on the surface of the metal are needed to control the process by suppressing electrochemical reactions, such as the use of inhibitors.

The use of environmentally friendly corrosion control methods has gained popularity among experts, in line with the international vision for a chemical additive-free world by 2030 [10]. Furthermore, a green inhibitor from natural materials that are biodegradable, safe, affordable, readily available, and environmentally friendly is at the core of study development by engineers and scientists [11]. Among the natural materials explored for corrosion inhibition are plant extracts from leaves, fruits, stems, and roots. These extracts often contain polar compounds, such as oxygen and nitrogen as well as non-polar compounds, including aromatic rings, aliphatic chains, and heterocyclic rings, which play a role in the adsorption and film formation processes on the metal's surface [12]. Based on these results, inhibitors from natural materials become ideal candidates to replace less environmentally friendly synthetic materials.

The application of natural materials as corrosion inhibitors has been extensively explored, such as the use of *Syzygium Cumini* seed extract in acidic environments [13] and *Syzygium Cumini* leaf extract for carbon steel in acidic media [14]. The use of *Syzygium Cumini* fruit is also prevalent in medical science, serving as an anti-cancer, anti-microbial, [15], anti-diabetic, and anti-toxicity agent [16]. Despite this extensive usage, there are no studies on its use as an anti-corrosion agent. The novelty of this report lies in using *Syzygium Cumini* fruit extract as a green inhibitor on low-carbon steel in a 3.5% NaCl solution. Previous studies have identified the presence of flavonoids, polyphenols, and tannins in the fruit of the plant, actively contributing to film formation [17] and suggesting significant potential as an anti-corrosion agent. Therefore, this study aims to (1) analyze the effectiveness of *Syzygium Cumini* fruit extract inhibitor performance based on the efficiency values and (2) evaluate the recent chemical transformation role of the fruit regarding its anti-corrosion effects through weight loss measurement and modeling, as well

as electrochemistry, including potentiodynamic polarization (PDP) and electrochemical impedance spectroscopy (EIS). The extract was characterized using Fourier Transfer Infrared Spectroscopy (FTIR) and phytochemical tests. The morphology of low carbon steel before and after protection by inhibitor was analyzed using Scanning Electron Microscope-Energy Dispersive X-ray (SEM-EDX) and X-ray diffraction (XRD).

2. Materials and Methods

2.1. Materials and electrolyte medium

The material used in this study was low carbon (AISI 1020) steel purchased in Banda Aceh, Indonesia. The sample was cut into dimensions of 3×2×0.3 cm for weight loss test and 1×1×0.5 cm, coated with resin, for electrochemical test. Furthermore, Table 1 provided insight into its chemical composition, classifying the specimen as low-carbon steel, with a carbon (C) content of 0.18%.

Table 1. Chemical composition of low carbon steel.

Element	C	Si	Mn	P	S	Cr	Mo	Ni	Cu	Al	Nb	Fe
Wt.%	0.18	0.26	1.25	0.03	0.03	0.15	0.03	0.09	0.28	0.01	0.01	Balance

The corrosive solution used was 3.5% NaCl, which was prepared by dissolving 3.5 grams of NaCl powder in 1 liter of distilled water.

2.2. Preparation of Syzygium Cumini fruit extract

The inhibitor used was *Syzygium Cumini* fruit extract obtained from Lamreh, Aceh Besar, Indonesia, and the extraction process was carried out using the solid-liquid method [18]. A total of 5 kilograms of *Syzygium Cumini* fruit were collected, dried at 50°C, crushed, and packed into a Soxhlet extractor using 1 liter of 96% Ethanol with three reflux cycles at 70°C. Furthermore, the solution was separated using a rotary evaporator at 60°C, and the extract was stored in glass bottles at room temperature.

2.3. FTIR analysis and phytochemical analysis

The chemical composition of *Syzygium Cumini* fruit extract was tested using FTIR analysis to identify functional groups present. The resulting functional groups played an active role in the formation of protective layers or films on the surface of carbon steel [19]. Furthermore, FTIR analysis was performed using a Shimadzu IR Prestige-21 infrared spectrophotometer with spectra ranging from 500 to 4000 cm^{-1}. Phytochemical analysis was carried out using 95% alcohol as an extractor to examine the chemical content of *Syzygium Cumini* fruit.

2.4. Weight loss method

The weight loss method was used to determine the corrosion rate of low-carbon steel and the efficiency of the *Syzygium cumini* fruit inhibitor. The carbon steel was immersed in a 3.5% NaCl solution and inhibitor mixtures at concentrations of 100, 200, 300, 400 and 500 ppm. Weight was measured before and after immersion, starting with surface cleaning. Furthermore, immersion was performed over an exposure time of 25 days, measured every 5 days (120, 240, 360, 480, and 600 hours). Corrosion rate and inhibitor efficiency were calculated based on Equations 1 and 2 [20]:

$$\text{Corrosion rate, CR } \left(\text{mm/year}\right) = \frac{87.6 \cdot W_{\text{L}}}{A \cdot T \cdot \rho} \tag{1}$$

$$\text{Inhibitor efficiency, } \eta\% = \frac{CR^{\text{free}} - CR^{\text{inh}}}{CR^{\text{free}}} \cdot 100\% \tag{2}$$

where W_{L} is weight loss (in mg), A is the surface area of carbon steel (in cm²), T is the immersion time (in hours), ρ is the density (in g/cm³), and CR^{free} and CR^{inh} are corrosion rate without and with the inhibitor.

2.5. Electrochemical studies

In this study, 2 electrochemical test methods were used, including potentiodynamic polarization (PDP) and EIS. A Zive Lab potentiostat model and IVMAN software were used for measurement. Furthermore, 3 electrodes, namely the counter electrode (graphite), low carbon steel as the working electrode (WE), and the reference electrode (Ag/AgCl). The working electrode was immersed for 30 minutes to reach a steady-state condition. The corrosion rate on carbon steel was calculated by adjusting the polarization curve using the Tafel analysis method, starting with determining corrosion potential (E_{corr}) and current density (i_{corr}). Corrosion rate measurement based on ASTM G102-89 with inhibitor efficiency was performed using the formula [21]:

$$I\% = \frac{CR_{\text{unh}} - CR_{\text{inh}}}{CR_{\text{unh}}} \cdot 100\% \tag{3}$$

where CR_{unh} and CR_{inh} are corrosion rates on carbon steel with and without the inhibitor (mpy). EIS measurement was conducted with an open circuit under AC amplitude of 10 mV and frequency ranging from 100 kHz to 10 mHz.

2.6. Surface analysis with SEM-EDX and XRD

SEM was used to scan the surface morphology of carbon steel. SEM analysis was a preferred choice in several studies due to its ability to visualize particles smaller than 10 nm [22]. Furthermore, EDX was used to identify elements present in carbon steel. EDX analysis could determine a histogram based on the number of particles produced on the

surface or determine the percentage composition of sample elements. XRD analysis was useful for showing diffraction results of X-rays in the form of nanoparticles, biomolecules, and polymers. Morphological analysis was performed on carbon steel before and after immersion in NaCl solution and *Syzygium Cumini* fruit inhibitor at a concentration of 500 ppm.

3. Results and Discussion

3.1. FTIR and phytochemical analysis

FTIR in Figure 1 represented the spectrum directly providing information about the functional groups present in *Syzygium Cumini* fruit extract. The generated spectrum showed prominent adsorption peaks useful for showing the chemical composition of the inhibitor. The adsorption band with the strongest intensity broadened at the peak of 3359.99 cm^{-1}, showing the presence of hydroxyl (O–H) stretching. Meanwhile, the adsorption band broadening at 2933.73 cm^{-1} showed Alkane (C–H) stretching with strong adsorption intensity. Carbonyl (C=O) bond stretching was scattered in the spectrum at 1724.36 cm^{-1}. In the FTIR spectrum, there was a moderate adsorption band at 1041.56 cm^{-1}, representing aromatic esters (C–H) bending.

The presence of functional groups containing heteroatoms, such as oxygen (O) and hydrogen (H) actively contributed to preventing corrosion on the surface of carbon steel by providing electron donations to form a protective film. This was reinforced by the presence of aromatic double bonds that played an active role in the adsorption process, making *Syzygium Cumini* fruit inhibitors effective as an anti-corrosion agent [23]. With the presence of heteroatoms and aromatic bonds, the corrosion rate on the surface of the sample could be reduced [24].

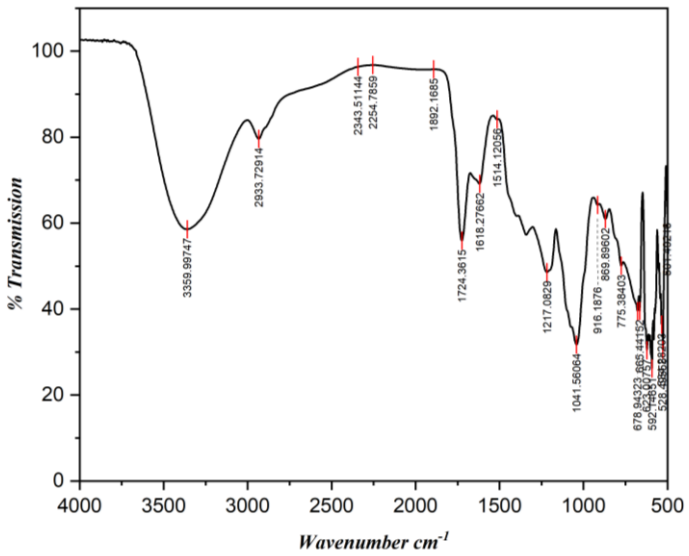

Figure 1. FTIR spectrum of *Syzygium cumini* fruit extract.

Table 2. Phytochemical of *Syzygium Cumini* fruit.

Chemical contents	Result	Description
Alkaloid	A white precipitate formed	+
Flavonoid	Dark red (magenta)	++
Phenol	Green or bluish-green	++
Glycoside	Blue or green	+
Saponin	Stable foam	+
Tannin	A blackish-green color formed	++
Steroid	Brownish ring	+
Triterpenoids	Red or purple	+

(++) high quantity, (+) low quantity

The phytochemical analysis results of *Syzygium Cumini* fruit are presented in Table 2, showing the presence of flavonoids marked in a dark red (magenta) color with a significant quantity. Furthermore, there were tannins marked in a blackish-green color in a substantial quantity. The chemical contents of flavonoids and tannins in *Syzygium Cumini* fruit were promising organic substances suitable for use as corrosion inhibitors for carbon steel in neutral media [25, 26].

3.2. Weight loss measurements

The influence of adding *Syzygium Cumini* fruit inhibitor on the corrosion rate of low-carbon steel was tested with different concentrations. The inhibitor efficiency percentage η% against corrosion rate was obtained after immersion for 25 days at room temperature (25±2°C), as shown in Table 3. Based on the results, the corrosion rate on carbon steel decreased proportionally with increasing inhibitor concentration from 100 to 500 ppm [27]. Furthermore, the parameter was determined based on the weight loss of carbon steel during the immersion process. The weight of carbon steel continued to decrease due to the corrosion process on the surface by the solution. The addition of the inhibitor to the corrosive solution led to minimal weight loss. The highest weight loss occurred in carbon steel immersed in a 3.5% NaCl solution without the inhibitor mixture. This was due to the absence of protection on the surface, exposing it directly to the corrosive environment [28].

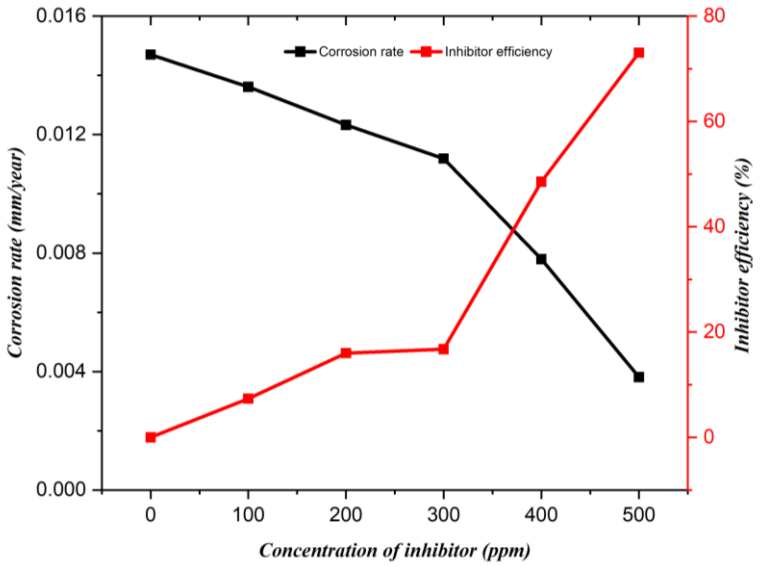

Figure 2. Comparison of corrosion rate and inhibitor efficiency in 3.5% NaCl solution at different concentrations.

Table 3. Inhibitor efficiency of *Syzygium Cumini* fruit on low carbon steel corrosion rate.

Inhibitor concentrations, ppm	**0**	**100**	**200**	**300**	**400**	**500**
Corrosion rate, mm/year	0.0147	0.0136	0.0123	0.0112	0.0078	0.0038
Inhibitor efficiency%	0.00	7.48	16.33	23.81	46.94	74.15

The greater mass loss of carbon steel in NaCl solution is a consequence of the increased corrosion rate. The corrosion rate decreased with the increasing concentration given, leading to the highest average efficiency value of 74.15% at a concentration of 500 ppm. This behavior was triggered by the phytochemical adsorption process of *Syzygium Cumini* fruit on the surface of carbon steel [29]. The formation of the protective layer is the process of electron donation from the natural extract inhibitor on the carbon steel surface when Fe^{+2} ions diffuse into the electrolyte solution and the attack of active Cl ions from the NaCl solution. Corrosion rate was calculated based on Equation 1 and the inhibitor efficiency was obtained after determining the parameter with and without the inhibitor. The lower the corrosion rate produced, the higher the inhibitor efficiency value, and vice versa. Figure 2 shows the comparison of efficiency with corrosion rate based on different inhibitor concentrations. The highest efficiency value at a concentration of 500 ppm proved the increased *Syzygium Cumini* fruit molecular composition, leading to the interaction of the inhibitor's chemical group with the surface of carbon steel.

3.3. Potentiodynamic Polarization Test (PDP)

The potentiodynamic polarization curve of low carbon steel in a corrosive 3.5% NaCl solution and a mixture of *Syzygium Cumini* fruit inhibitor with various concentrations at

room temperature (25±2°C) is shown in Figure 3. Corrosion performance could be observed based on kinetic parameters found in Table 4, such as corrosion potential (E_{corr}) and current density (i_{corr}), covering corrosion rate to yield inhibitor efficiency. According to the test results, the current density value (i_{corr}) decreased according to the anodic, cathodic, and potentiodynamic polarization curve graphs. It also decreased with the increasing quantity of *Syzygium Cumini* fruit inhibitor concentrations [30]. This analysis proved that the presence of the inhibitor influenced the surface of carbon steel by undergoing adsorption to inhibit anodic and cathodic processes [31].

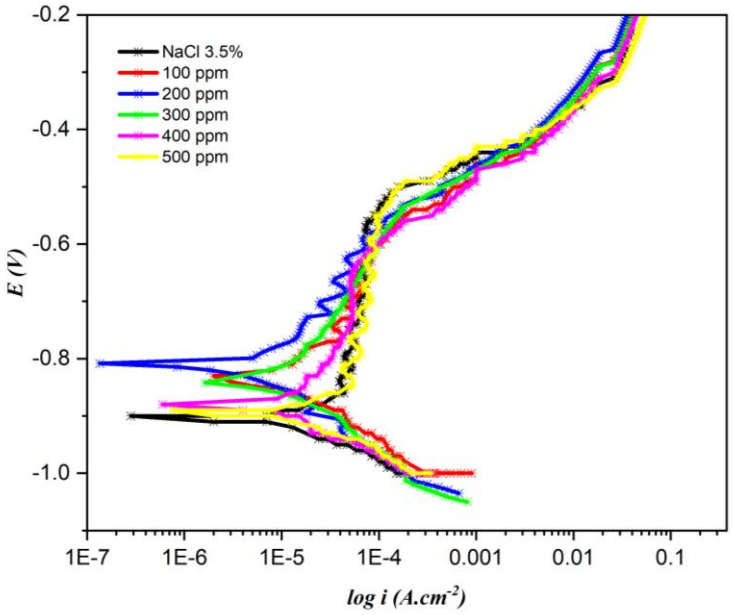

Figure 3. Polarization curve of low carbon steel in 3.5% NaCl solution and *Syzygium Cumini* fruit inhibitor mixture.

The corrosion rate from the electrochemical test was obtained based on a potentiodynamic polarization curve with intersections in the anodic and cathodic regions on the current density (i_{corr}) and corrosion potential (E_{corr}) coordinate axes. Electrochemical parameters in Table 4 showed that the highest current density (i_{corr}) occurred in the NaCl solution because there was no protection on the surface of carbon steel. The high current density (i_{corr}) led to an increase in the corrosion rate of carbon steel. The addition of the inhibitor to the NaCl corrosive solution significantly influenced the corrosion rate. Current density decreased significantly with the lowest value of 3.8 μm/cm^2 at an inhibitor concentration of 500 ppm, thereby reducing the parameter. The highest inhibitor efficiency reached 92.99%, showing that the active substances and functional groups in the *Syzygium Cumini* fruit were polar compounds that played an active role in handling carbon steel corrosion. Moreover, the addition of the inhibitor provided a reaction on the surface by forming a film in the form of a solid or reticulated layer, serving as a good anti-corrosion agent [32].

Table 4. Electrochemical parameters of polarization curves for low carbon steel in 3.5% NaCl solution and *Syzygium Cumini* fruit inhibitor.

Inhibitor, ppm	β_a, V/div	β_c, V/div	I_{corr}, µm/cm^2	E_{corr}, mV	kOhm	Corrosion rate, mm/y	PDP η%
NaCl	2.67	0.18	53.9	–907.7	1.35	0.628	0.00
100	0.24	0.17	16.7	–826.7	2.61	0.194	69.11
200	0.36	0.15	14.6	–810.6	3.20	0.169	73.09
300	0.22	0.12	9.5	–838.1	3.24	0.111	82.32
400	0.16	0.08	8.9	–883.2	2.42	0.104	83.44
500	0.07	0.04	3.8	–892.3	2.30	0.044	92.99

3.4. Electrochemical impedance spectroscopy (EIS)

The influence of *Syzygium Cumini* fruit inhibitor concentration on impedance treatment of low carbon steel in 3.5% NaCl corrosive solution was analyzed using the EIS method. Impedance data were shown in the form of a Nyquist diagram, bode plot, which was presented in Figure 4. The EIS test was carried out on the solution with different inhibitor concentrations, namely without and with 100, 200, 300, 400, and 500 ppm inhibitors at room temperature (25±2°C).

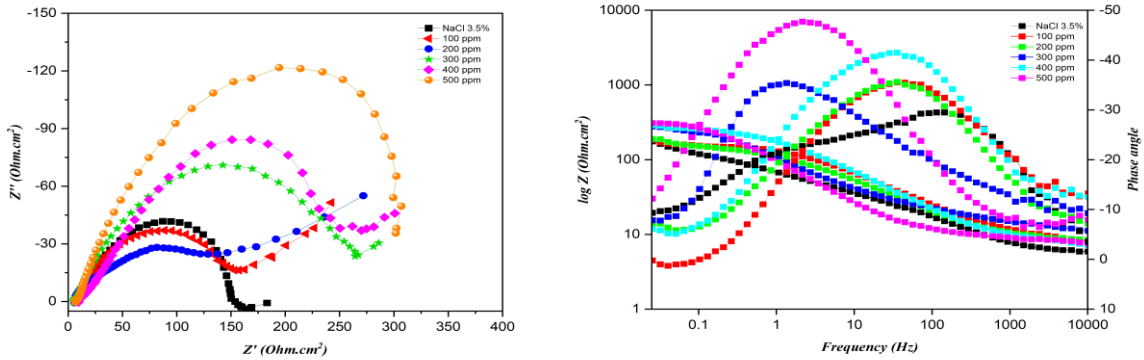

(a) (b)

Figure 4. Nyquist diagram (a) bode plot (b) of low carbon steel in 3.5% NaCl solution and *Syzygium Cumini* fruit inhibitor mixture.

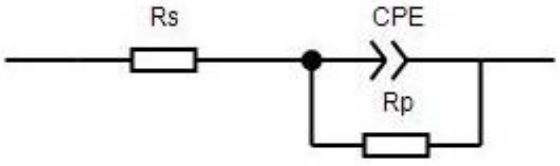

Figure 5. Equivalent circuit model on low carbon steel with *Syzygium Cumini* fruit inhibitor.

Impedance spectra was simulated with two equivalent circuits that could be seen in Figure 5, where the EIS fitting circuit with and without inhibitor consisted of three circuit constituent variables, namely R_s as the solution resistance, R_p as the charge transfer resistance, and CPE as a phase constant element. The equivalent circuit model formed was a parallel form between R_p and CPE, while R_s formed a series circuit against R_p and CPE, and the values of the EIS test parameters were shown in Table 5. The Nyquist diagram consisted of two capacitive loops located at high and intermediate frequency positions preceded by an inductive loop region at a lower frequency. The loops in the Nyquist diagram expressed high or low corrosion rate values [33]. Figure 4 showed that the variety of loop shapes corresponded to the shape and surface condition of the carbon steel. The Nyquist diagram increased significantly with the increase in concentration given to the corrosive solution of 100 to 500 ppm. This process could be related to the adsorption process by chemical substances from the *Syzygium cumini* fruit inhibitor, which played an active role in the electrode transfer process on the surface of low-carbon steel. Furthermore, this evidence was reinforced by the bode diagram, where the bode modulus and phase angle increased along with the corrosion inhibitor.

The parameters of the Nyquist diagram showed that carbon steel without inhibitor produced a charge transfer resistance (R_p) value of 167.05. With the addition of an inhibitor, the charge transfer resistance value (R_p) increased [34] by 194.76, 243.71, 304.33, 375.94, and 384.71 ($\Omega \cdot cm^2$) at 100, 200, 300, 400, and 500 ppm, respectively. The increased value of the parameter showed that the *Syzygium Cumini* fruit inhibitor influenced the charge transfer on the surface of the sample. The addition of the inhibitor provided a film-shaped protective layer on the surface of low-carbon steel. The efficiency value of *Syzygium cumini* fruit inhibitor could be calculated using Equation 4 [35].

$$E\% = \frac{R_p - R_{p0}}{R_p} \cdot 100\% \quad (4)$$

where R_p and R_{p0} are the charge transfer resistance values with and without the inhibitor mixture. The highest inhibitor efficiency value was obtained at a concentration of 500 ppm, showing that the data obtained in the EIS test was appropriate to weight loss and potentiodynamic polarization data [13].

Table 5. EIS parameters for low carbon steel in 3.5% NaCl solution and *Syzygium Cumini* fruit inhibitor.

Inhibitor, ppm	R_s, $\Omega \cdot cm^2$	R_p, $\Omega \cdot cm^2$	CPE-T	CPE-P	E_{EIS}%
0	6.48	167.05	$1.1469 \cdot 10^{-3}$	$5.6557 \cdot 10^{-1}$	0
100	7.24	194.76	$1.9436 \cdot 10^{-3}$	$5.4084 \cdot 10^{-1}$	14.23
200	4.91	243.71	$5.0477 \cdot 10^{-3}$	$4.3454 \cdot 10^{-1}$	31.46
300	5.92	304.33	$1.1838 \cdot 10^{-3}$	$5.8555 \cdot 10^{-1}$	45.11
400	7.75	375.94	$2.8251 \cdot 10^{-3}$	$6.5635 \cdot 10^{-1}$	55.56
500	10.22	384.71	$3.2822 \cdot 10^{-3}$	$4.8699 \cdot 10^{-1}$	56.58

3.4.1. Scanning electron microscopy (SEM)

SEM was used to analyze the morphology of the carbon steel surface, as shown in Figure 6. The carbon steel surface was tested in conditions before immersion and after being immersed for 25 days in a 3.5% NaCl corrosive solution and a mixture of 500 ppm *Syzygium Cumini* fruit inhibitor. Based on the image, the sample before immersion (Figure 6a) did not undergo corrosion and experience damage. Compared to carbon steel after immersion, high corrosion levels were observed in carbon steel in the 3.5% NaCl solution (Figure 6b). The lack of surface protection exposed the sample directly to the corrosive environment, where the surface appeared rough and covered with corrosion products. The solution without an inhibitor caused the oxidation process to occur, leading to significantly faster corrosion. The carbon steel surface appeared smoother, with very little corrosion formation and minimal damage after immersion in the 500 ppm inhibitor mixture (Figure 6c). Surface protection of low-carbon steel was based on the formation of a film layer by the *Syzygium Cumini* fruit inhibitor. The formation of the film layer by inhibitor components actively contributed to reducing the corrosion rate [36]. The observed activity proved that the *Syzygium Cumini* fruit inhibitor significantly contributed to the mechanism of natural chemicals as an anti-corrosion agent. The formation of a barrier layer showed the occurrence of a good adsorption process by the inhibitor, thereby reducing the oxidation-reduction reactions and slowing down the corrosion of carbon steel [37].

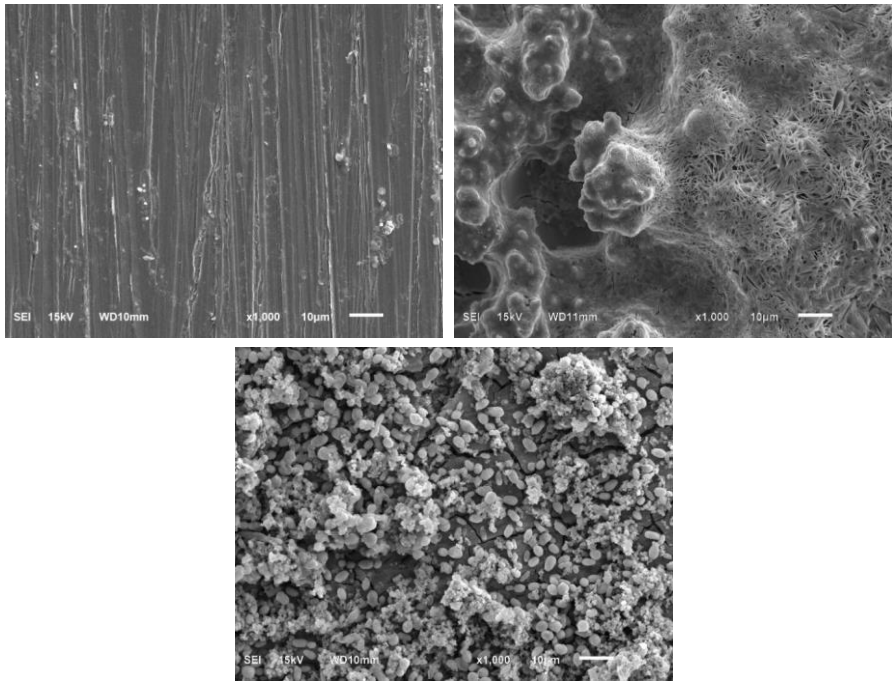

Figure 6. Low carbon steel before immersion (a) after immersion with 3.5% NaCl solution (b) after soaking with 500 ppm mixture of *Syzygium Cumini* fruit inhibitor (c).

3.4.2. EDX Analysis

EDX Analysis was performed to examine the chemical composition of the carbon steel surface. The results, in the form of the percentage of chemical elements in carbon steel, could be determined based on the EDX spectrum level. The characterization ability of elements was mainly due to the basic principle that each element had a unique atomic structure that allowed for specific peaks in its electromagnetic emission spectrum, which was the main principle of spectroscopy.

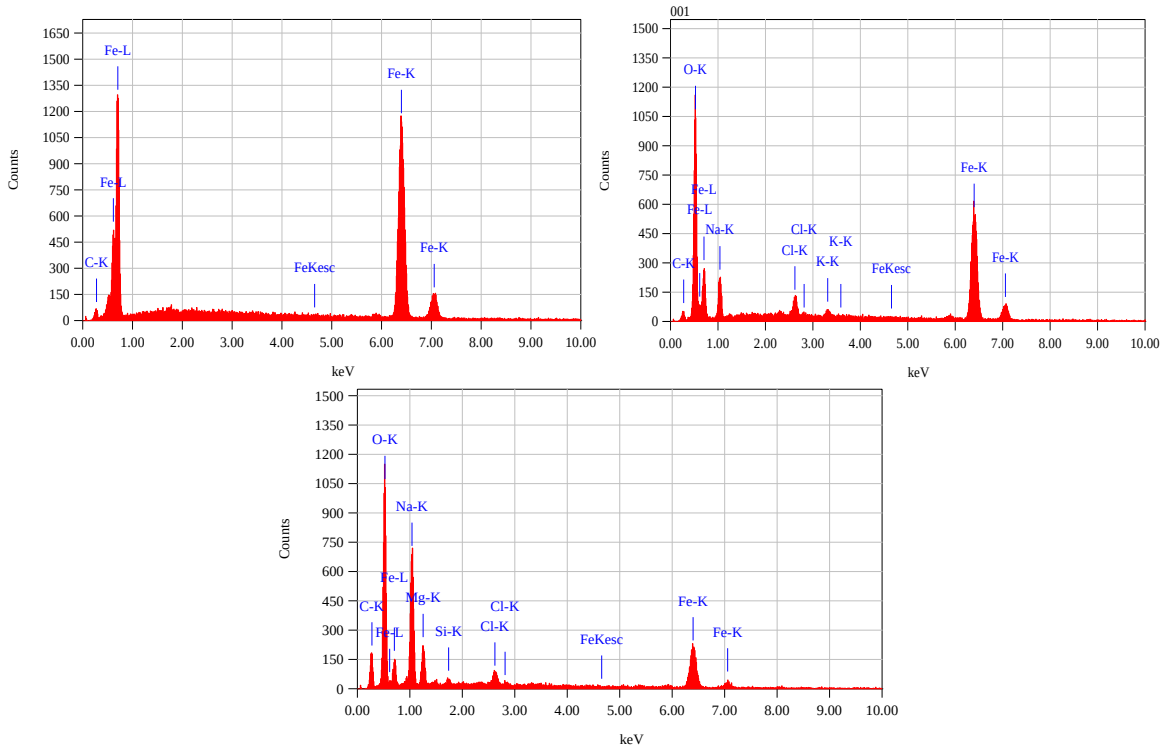

Figure 7. EDX analysis of low carbon steel before immersion (a) after immersion in 3.5% NaCl (b) after immersion in 500 ppm *Syzygium Cumini* fruit inhibitor mixture (c).

The composition of carbon steel elements was indexed with the EDX spectrum in Figure 7, and the percentage of chemical composition was shown in Table 6. The results showed that before immersion, carbon steel showed iron (Fe) and carbon (C) content at 95.66% and 4.43%, respectively. After immersion, the carbon steel surface showed carbon (C) at 4.20%, iron (Fe) at 60.10%, and the emergence of oxygen (O) chemical elements at 28.03%, sodium (Na) at 6.51%, chloride (Cl) at 1.72%, and potassium (K) at 0.75%. Carbon steel immersed in a corrosive solution mixed with *Syzygium Cumini* fruit inhibitor at a concentration of 500 ppm has a percentage of iron (Fe) at 25.32% and chloride (Cl) at 1.31%, leading to a decrease in percentage influenced by the film layer covering the Fe layer. The oxygen (O) content was 37.55%, and the carbon (C) content was 17.93%, showing an increase in percentage in the inhibitor mixture. The appearance of oxygen (O) elemental groups proved that the corrosion control process comprised electron contribution by the inhibitor as a protective layer [38]. The reaction showed that a corrosion barrier

layer was formed on the carbon steel surface from the adsorption process of the *Syzygium Cumini* fruit inhibitor on the carbon steel surface [39]. Therefore, *Syzygium Cumini* fruit played a significant role as a good inhibitor in NaCl corrosive solution.

Table 6. Surface composition of carbon steel elements before immersion, immersion in 3.5% NaCl, and concentration of 500 ppm by EDX analysis.

Element	Before immersion		NaCl 3.5%		500 ppm	
	Wt.%	Atomic %	Wt.%	Atomic %	Wt.%	Atomic %
C	4.34	17.43	4.20	10.08	17.93	29.30
O	–	–	28.03	50.46	37.55	46.06
Na	–	–	5.19	6.51	13.77	11.75
Mg	–	–	–	–	3.60	2.91
Si	–	–	–	–	0.52	0.36
Cl	–	–	1.72	1.40	1.31	0.73
K	–	–	0.75	0.56	–	–
Fe	95.66	82.57	60.10	31.00	25.32	8.90

3.5. XRD Analysis

XRD Analysis was necessary as it was related to the characterization of a material or solid substance. Most solid substances formed crystals classified into 7 crystal systems and divided into 14 lattices. At lattice points, crystal planes were formed and expressed with Miller indices. Materials diffracted with X-rays showed their crystal systems, such as SC, BCC, and FCC. X-rays were used to determine the characteristics of materials and are often obtained by shooting electrons from an electron source at a target atom. From the Miller indices, the atomic radii were then determined, leading to a crystal structure.

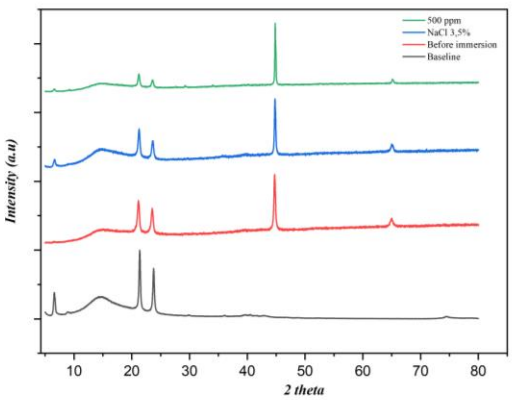

Figure 8. XRD graph of low carbon steel before exposure, after exposure to 3.5% NaCl and *Syzygium Cumini* fruit inhibitor mixture.

The results of XRD testing are presented in Figure 8. XRD was conducted on low-carbon steel before and after exposure to 3.5% NaCl, and carbon steel immersed in a corrosive solution with a mixture of inhibitors at a concentration of 500 ppm. The XRD results in Figure 10 showed changes in peaks based on intensity and 2θ due to different treatments on the sample. The results in Figure 10 showed that low-carbon steel, before immersion, produced peaks at 44.71° on the (1 1 0) Miller index plane and peaks at 65.08° on the (2 0 0) Miller index plane. After exposure to NaCl solution, it produced peaks at 44.77° on the (1 1 0) Miller index plane and peaks at 65.17° with the (2 0 0) Miller index. Peaks were produced at 44.78° on the (1 1 0) Miller index plane and at 65.18° on the (2 0 0) Miller index after immersion with the inhibitor mixture. XRD results in Figure 10 proved that a *Syzygium Cumini* fruit inhibitor mixture increased the intensity of index peaks and decreased the crystalline index on low carbon steel by 17.30% compared to NaCl 23.73% and before immersion by 27.90% [40].

4. Conclusion

In conclusion, this study showed that the use of *Syzygium Cumini* Fruit extract as an inhibitor provided good corrosion protection for low carbon steel in a 3.5% NaCl solution. This was evidenced through weight loss testing, electrochemistry (PDP and EIS), and surface morphology analysis of the sample. Weight loss results showed that the lowest corrosion rate occurred at a concentration of 500 ppm. Furthermore, PDP showed that the addition of the inhibitor successfully reduced the current density (i_{corr}) as the inhibitor concentration increased. Based on the EIS analysis, the higher the inhibitor concentration, the higher the charge transfer resistance (R_p), specifically at a concentration of 500 ppm. This was accompanied by the formation of a higher loop compared to the NaCl corrosive solution and an increase in the bode modulus and phase angle. The morphologies from SEM-EDX and XRD analyses explained the occurrence of minimal damage, evidenced by the protection of the carbon steel surface layer and the adsorption of chemically active substances. Therefore, it was concluded that the inhibitor from *Syzygium Cumini* fruit extract was an ideal candidate as a corrosion inhibitor and an alternative green inhibitor to synthetic materials.

Acknowledgments

The authors are grateful to Universitas Syiah Kuala, Indonesia, for the financial support provided by the Professorial Research Assignment Agreement Letter *(Surat Perjanjian Penugasan Pelaksanaan Penelitian Profesor (PP)* Fiscal Year 2023 Number: (33/UN11.2.1/PT.01.03/PNBP/2023 dated May 3, 2023).

References

1. N. Ali and M.A. Fulazzaky, The empirical prediction of weight change and corrosion rate of low-carbon steel, *Heliyon*, 2020, **6**, e05050. doi: 10.1016/j.heliyon.2020.e05050
2. N.H.J. Al Hasan, H.J. Alaradi, Z.A.K. Al Mansor and A.H.J. Al Shadood, The dual effect of stem extract of Brahmi(Bacopamonnieri) and Henna as a green corrosion inhibitor for low carbon steel in 0.5 M NaOH solution, *Case Stud. Constr. Mater*., 2019, **11**, e00300. doi: 10.1016/j.cscm.2019.e00300
3. N. Ali, T.E. Putra, V.Z. Iskandar and M. Ramli, A simple empirical model for predicting weight loss of mild steel due to corrosion in NaCl solution, *Int. J. Automot. Mech. Eng*., 2020, **7**, 7784–7791. doi: 10.15282/ijame.17.1.2020.24.0579
4. W. Wang, Z. Yu, Y. Cui, R. Liu, L. Liu, Sh. Geng and F. Wang, Revealing of corrosion behavior of GH4169 under the alternate environment of intermediate temperature NaCl spraying and marine atmosphere, *J. Mater. Res. Technol*., 2023, **22**, 2316–2327. doi: 10.1016/j.jmrt.2022.12.081
5. C. Zhao, K. Dai, P. Li, Z. Cheng and K. Xiao, Effect of UV Illumination on the Corrosion Behavior of Under a Thin NaCl Electrolyte Layer, *Int. J. Electrochem. Sci*., 2022, **17**, 221164. doi: 10.20964/2022.11.80
6. W. Bao, T. Xiang, J. Chen, P. Du, Z. Zhang and G. Xie, Corrosion behavior of high-performance crystalline CuCrZr/amorphous CuZrAl composites in NaCl solution, *J. Mater. Res. Technol*., 2022, **21**, 5004–5017. doi: 10.1016/j.jmrt.2022.11.104
7. J. Cheng, Y. Wu, S. Zhu, S. Hong, J. Cheng and Y. Wang, The coupling effect of cavitation-erosion and corrosion for HVOF sprayed Cu-based medium-entropy alloy coating in 3.5 wt.% NaCl solution, *J. Mater. Res. Technol*., 2023, **25**, 2936–2947. doi: 10.1016/j.jmrt.2023.06.109
8. J. Phother-Simon, I. Hanif, J. Liske and T. Jonsson, The influence of a KCl-rich environment on the corrosion attack of 304 L: 3D FIB/SEM and TEM investigations, *Corros. Sci*., 2021, **83**, 109315. doi: 10.1016/j.corsci.2021.109315
9. L.K.M.O. Goni and M.A.J. Mazumder, *Green Corrosion Inhibitors*, Intech, 2019, **34**, 57–67. doi: 10.5772/intechopen.81376
10. V. Vorobyova, M. Skiba and E. Gnatko, Agri-food wastes extract as sustainable-green inhibitors corrosion of steel in sodium chloride solution: A close look at the mechanism of inhibiting action, *S. Afr. J. Chem. Eng*., 2023, **43**, 273–295. doi: 10.1016/j.sajce.2022.11.004
11. R.G.M. de A. Macedo, N. do N. Marques, J. Tonholo and R. de C. Balaban, Water-soluble carboxymethylchitosan used as corrosion inhibitor for carbon steel in saline medium, *Carbohydr. Polym*., 2018, **205**, 371–376. doi: 10.1016/j.carbpol.2018.10.081
12. N. Hossain, M.A. Chowdhury, M. Rana, M. Hassan and S. Islam, Terminalia arjuna leaves extract as green corrosion inhibitor for mild steel in HCl solution, *Results Eng*., 2022, **14**, 100438. doi: 10.1016/j.rineng.2022.100438

13. A. Singh and M.A. Quraishi, The extract of Jamun (Syzygium cumini) seed as green corrosion inhibitor for acid media, *Res. Chem. Intermed*., 2015 **41**, 2901–2914. doi: 10.1007/s11164-013-1398-3
14. M.V.L. da Silva, E. de B. Policarpi and A. Spinelli, Syzygium cumini leaf extract as an eco-friendly corrosion inhibitor for carbon steel in acidic medium, *J. Taiwan Inst. Chem. Eng*., 2021, **129**, 342–349. doi: 10.1016/j.jtice.2021.09.026
15. N.K. Kadiyala, B.K. Mandal, S. Ranjan and N. Dasgupta, Bioinspired gold nanoparticles decorated reduced graphene oxide nanocomposite using Syzygium cumini seed extract: Evaluation of its biological applications, *Mater. Sci. Eng. C*, 2018, **93**, 191–205. doi: 10.1016/j.msec.2018.07.075
16. E. Masaenah B. Elya, H. Setiawan, Z. Fadhilah, F. Wediasari, G.A. Nugroho, Elfahmi and T. Mozef, Antidiabetic activity and acute toxicity of combined extract of Andrographis paniculata, Syzygium cumini, and Caesalpinia sappan, *Heliyon*, 2021, **7**, e08561. doi: 10.1016/j.heliyon.2021.e08561
17. P.K. Dissanayake, W.G.C. Wekumbura, A.W. Wijeratne and D.S.A. Wijesundara, Morphological characterization, antioxidant capacity and diversity of Syzygium cumini trees from Sri Lanka, *Hortic. Plant J*., 2022, **8**, 53–67. doi: 10.1016/j.hpj.2021.09.002
18. F. Zhang, S. Deng, G Wei and X. Li, Alternanthera philoxeroides extract as a corrosion inhibitor for steel in Cl3CCOOH solution, *Int. J. Electrochem. Sci*., 2023, **18**, 100057. doi: 10.1016/j.ijoes.2023.100057
19. Ayende, R. Riastuti, J.W. Soedarsono, A.P.S. Kaban, M.I. Hikmawan and R.T. Rahmdani, Development of Annona Muricata Linn As Green Corrosion Inhibitor Under Produced Water: Inhibition Performance and Adsorption Model, *East.-Eur. J. Enterp. Technol*., 2023, **3**, 56–65. doi: 10.15587/1729-4061.2023.278911
20. G.K. Shamnamol, P. Rugma, S. John and J.M. Jacob, Unraveling the synergistic effect of cationic and anionic salt on the corrosion inhibition performance of Garcinia gummi-gutta leaf extract against mild steel in HCl medium, *Results Chem*., 2023, **5**, 100728. doi: 10.1016/j.rechem.2022.100728
21. M.A. Chowdhury, M.M.S. Ahmed, N. Hossain, M.A. Islam, S. Islam and M.M. Rana, Tulsi and green tea extracts as efficient green corrosion inhibitor for the corrosion of aluminum alloy in acidic medium, *Results Eng*., 2023, **17**, 100996. doi: 10.1016/j.rineng.2023.100996
22. K.C. Hembram, R. Kumar, L. Kandha, P.K. Parhi, C.N. Kundu, and B.K. Bindhani, Therapeutic prospective of plant-induced silver nanoparticles: application as antimicrobial and anticancer agent, *Artif. Cells, Nanomed., Biotechnol*., 2018, **46**, 38–51. doi: 10.1080/21691401.2018.1489262
23. M.A. Quraishi and R. Sardar, Aromatic Triazoles as Corrosion Inhibitors for Mild Steel in Acidic Environments, 2002, **58**, 748–755. doi: 10.5006/1.3277657

24. O.D. Olakolegan, S.S. Owoeye, E.A. Oladimeji and O.T. Sanya, Green synthesis of Terminalia Glaucescens Planch (Udi plant roots) extracts as green inhibitor for aluminum (6063) alloy in acidic and marine environment, *J. King Saud Univ. - Sci*., 2020, **32**, 1278–1285. doi: 10.1016/j.jksus.2019.11.010
25. T. Sithuba, N.D. Masia, J. Moema, L.C. Murulana, G. Masuku, I. Bahadur and M.M. Kabanda, Corrosion inhibitory potential of selected flavonoid derivatives: Electrochemical, molecular Zn surface interactions and quantum chemical approaches, *Results Eng*., 2022, **16**, 100694. doi: 10.1016/j.rineng.2022.100694
26. V. Vorobyova, O. Sikorsky, M. Skiba and G. Vasyliev, Quebracho tannin as corrosion inhibitor in neutral media and novel rust conversion agent for enhanced corrosion protection, *S. Afr. J. Chem. Eng*., 2023, **44**, 68–80. doi: 10.1016/j.sajce.2023.01.003
27. C. Kamal and M.G. Sethuraman, Spirulina platensis - A novel green inhibitor for acid corrosion of mild steel, *Arab. J. Chem*., 2012, **5**, 155–161. doi: 10.1016/j.arabjc.2010.08.006
28. P. Muthukrishnan, P. Prakash, B. Jeyaprabha and K. Shankar, Stigmasterol extracted from Ficus hispida leaves as a green inhibitor for the mild steel corrosion in 1 M HCl solution, *Arab. J. Chem*., 2019, **12**, 3345–3356. doi: 10.1016/j.arabjc.2015.09.005
29. T.A.S. Guimarães J.N. da Cunha, G.A. de Oliveira, T.U. da Silva, S.M. de Oliveira, J.R. de Araújo, S. de P. Machado, E. D'Elia and M.J.C. Rezende, Nitrogenated derivatives of furfural as green corrosion inhibitors for mild steel in HCl solution, *J. Mater. Res. Technol*., 2020, **9**, 7104–7122. doi: 10.1016/j.jmrt.2020.05.019
30. M.B. Harb, S. Abubshait, N. Etteyeb, M. Kamoun and A. Dhouib, Olive leaf extract as a green corrosion inhibitor of reinforced concrete contaminated with seawater, *Arab. J. Chem*., 2020, **13**, 4846–4856. doi: 10.1016/j.arabjc.2020.01.016
31. I.B. Obot, N.K. Ankah, A.A. Sorour, Z.M. Gasem and K. Haruna, 8-Hydroxyquinoline as an alternative green and sustainable acidizing oilfield corrosion inhibitor, *Sustain. Mater. Technol*., 2017, **14**, 1–10. doi: 10.1016/j.susmat.2017.09.001
32. C. Verma, M.A. Quraishi and N.K. Gupta, 2-(4-{[4-Methyl-6-(1-methyl-1H-1,3-benzodiazol-2-yl)-2-propyl-1H-1,3-benzodiazol-1-yl] methyl} phenyl) benzoic acid as green corrosion inhibitor for mild steel in 1 M hydrochloric acid, *Ain Shams Eng. J*., 2018, **9**, 1225–1233. doi: 10.1016/j.asej.2016.07.003
33. N. Dindodi and A.N. Shetty, Stearate as a green corrosion inhibitor of magnesium alloy ZE41 in sulfate medium, *Arab. J. Chem*., 2019, **12**, 1277–1289. doi: 10.1016/j.arabjc.2014.11.028
34. R.S. Nathiya and V. Raj, Evaluation of Dryopteris cochleata leaf extracts as green inhibitor for corrosion of aluminium in 1 M H2SO4, *Egypt. J. Pet*., 2017, **26**, 313–323. doi: 10.1016/j.ejpe.2016.05.002
35. X. Liu, Y. Gao, J. Guan, Q. Zhang, Yu Lin, Ch. Shi, Y. Wang, J. Du and N. Ma, Corrosion inhibition properties of spinach extract on Q235 steel in a hydrochloric acid medium, *Arab. J. Chem*., 2023, **16**, 105066. doi: 10.1016/j.arabjc.2023.105066

36. H.A. Abdullah, R.A. Anaee, A.A. Khadom, A.T. Abd, A.H. Malik and M.M. Kadhim, Results in Chemistry Experimental and theoretical assessments of the chamomile flower extract as a green corrosion inhibitor for aluminum in artificial seawater, *Results Chem*., 2023, **6**, 101035. doi: 10.1016/j.rechem.2023.101035
37. M.R. Singh, P. Gupta and K. Gupta, The litchi (Litchi Chinensis) peels extract as a potential green inhibitor in prevention of corrosion of mild steel in 0.5 M H_2SO_4 solution, *Arab. J. Chem*., 2019, **12**, 1035–1041. doi: 10.1016/j.arabjc.2015.01.002
38. E. Ituen, A. Singh, L. Yuanhua and O. Akaranta, Biomass-mediated synthesis of silver nanoparticles composite and application as green corrosion inhibitor in oilfield acidic cleaning fluid, *Clean. Eng. Technol*., 2021, **3**, 100119. doi: 10.1016/j.clet.2021.100119
39. A.I. Ikeuba, O.B. John, V.M. Bassey, H. Louis, A.U. Agobi, J.E. Ntibi and F.C. Asogwa, Experimental and theoretical evaluation of Aspirin as a green corrosion inhibitor for mild steel in acidic medium, *Results Chem*., 2022, **4**, 100543. doi: 10.1016/j.rechem.2022.100543
40. M.A. Chowdhury, N. Hossain, M.M.S. Ahmed, M.A. Islam, S. Islam and M.M. Rana, Green tea and tulsi extracts as efficient green corrosion inhibitor for aluminum alloy in alkaline medium, *Heliyon*, 2023, **9**, E16504. doi: 10.1016/j.heliyon.2023.e16504

♦ ♦ ♦